JOURNAL OF CATALYSIS **151**, 385–393 (1995)

The Effect of Alumina Phase Structure on the Dispersion of Rhodium/Alumina Catalysts

R. W. McCabe, R. K. Usmen, K. Ober, and H. S. Gandhi

Ford Research Laboratory, Ford Motor Company, Dearborn, Michigan 48121

Received July 1, 1994; revised October 12, 1994

Aluminas from various sources were thermally treated in air to obtain a range of phases (δ, θ, and α) with BET surface areas between 5 and 90 m^2/g. Rhodium was impregnated onto the aluminas at a constant loading of 0.6 μmol Rh/m^2 (BET). The resultant Rh–Al_2O_3 catalysts were hydrothermally aged by treating in 10% H_2O/air at 1223 K for 24 h. Temperature-programmed reduction and a noble metal surface area measurement based on methanation of adsorbed CO were used to characterize the state of the Rh after aging. Three broad forms of Rh were identified: occluded, strongly interacted, and noninteracted. Apparent dispersions ranged from 3 to 11%, with the highest values obtained for α-alumina. A pronounced loading effect was observed for the Rh/α-alumina catalysts; dispersions ca. 10% were obtained only on samples with loadings less than about 1 μmol Rh/m^2 (BET). Higher loadings (>1.5 μmol Rh/m^2 (BET)) resulted in apparent dispersions of 3% or less. These results suggest that the most effective way to maximize the Rh dispersion in high-temperature aged alumina-based automotive catalysts is to isolate the Rh on α-phase alumina at loadings less than 1 μmol/m^2 (BET). Presteaming of selected aluminas at 1223 K for 24 h prior to Rh impregnation decreased the BET surface area and resulted in less occlusion of Rh during subsequent aging.

INTRODUCTION

A number of studies have examined the interaction between Rh and alumina which occurs at high temperatures in oxidizing environments (1–15). Scientific and practical interest in this interaction is keen because it represents the most important deactivation mode for Rh-containing three-way automotive catalysts. Early studies carried out at Ford Motor Company examined the role of the support in the high-temperature deactivation of Rh catalysts. Both γ- and δ-phase aluminas showed strong interactions with Rh at temperatures above 873 K (1), while α-alumina and zirconia showed weak interactions with Rh even after oxidizing treatments up to 1173 K (2). The latter observations were the basis for patents issued to Ford for automotive catalysts containing Rh on α-alumina- and zirconia-coated substrates (3, 16).

The objective of the present study is to systematically investigate the effect of the alumina phase structure on the extent of the interaction with Rh. One of the potential concerns with α-alumina as a support is that the absence of strong interactions with Rh could lead to enhanced sintering rates of the Rh as compared to catalysts using transitional alumina phases, particularly in high-temperature steam aging environments such as automotive exhaust. Thus, a hypothetical scenario can be constructed where at one extreme the Rh is strongly deactivated by interactions with the high surface area γ-alumina support while, at the other extreme, the Rh particles sinter excessively on low surface area α-alumina. The optimum alumina phase would lie somewhere in between, perhaps in either the δ- or θ-phase regions, where conceivably neither interaction with the support nor Rh particle sintering would be excessive. To address this possibility we undertook a program to carefully prepare a series of aluminas with various phases and BET areas, ranging from δ-phase aluminas with BET areas near 90 m^2/g to predominantly θ-phase aluminas with BET areas near 20 m^2/g and α-aluminas with BET areas near 7 m^2/g. The catalysts were loaded with 0.6 μmol Rh/m^2 (BET) to achieve a constant surface density of Rh in the fresh state despite the widely different surface areas of the aluminas. The catalysts were then hydrothermally aged at 1223 K in a 10% steam/air atmosphere, after which temperature-programmed reduction (TPR) and metal surface area measurements were carried out to determine the amount of Rh strongly interacted with the alumina support and also the fraction of exposed Rh atoms.

The results of these experiments confirm earlier studies which suggested that the α-phase of alumina is optimal for preserving the greatest fraction of exposed Rh atoms after high-temperature aging. The superiority of the α-phase is contingent, however, on starting with dilute surface concentrations of Rh, <1 μmol Rh/m^2

0021-9517/95 $6.00

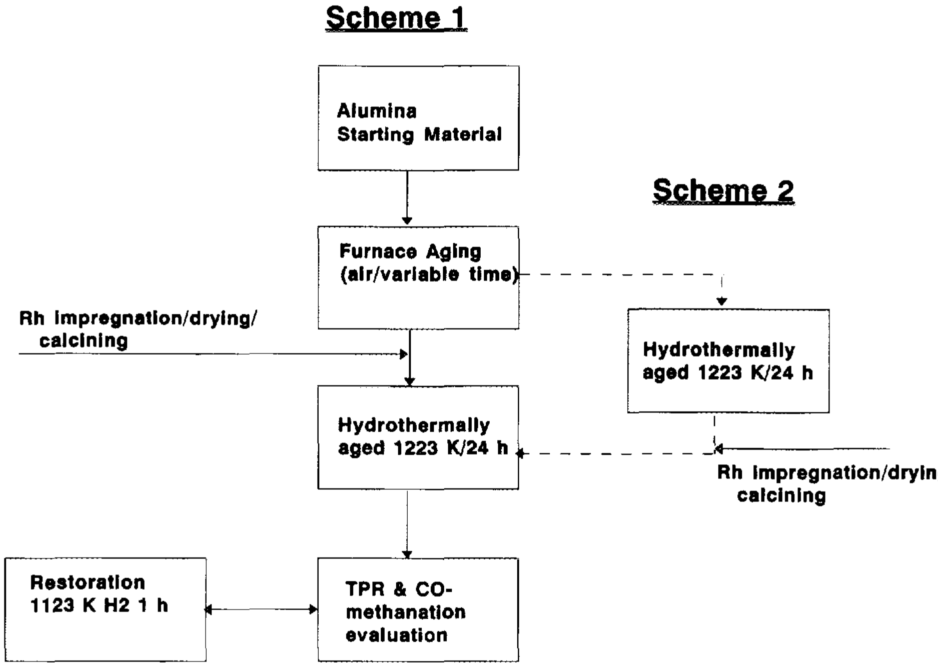

FIG. 1. Catalyst preparation and aging schemes. (Note that scheme 2 aging involves *two* 1223 K/24 h hydrothermal agings of the alumina—one before Rh impregnation and one after.)

(BET), which for a typical α-alumina translates into a weight loading of about 0.07%.

EXPERIMENTAL

Sample Preparation

The samples were prepared following the schemes shown in Figure 1. Various aluminum oxide powders (Degussa C, Alcoa, and Engelhard) were aged in air in a furnace at different temperatures and for various durations (Table 1) to obtain a range of Al_2O_3 phases. Each alumina sample was stirred in water and impregnated with a $Rh(NO_3)_3 \cdot 2H_2O$ solution at a concentration adjusted to give a normalized Rh loading of 0.6 μmol Rh/m^2 (BET). The catalyst samples were first dried at room temperature, then at 373 K, and subsequently calcined at 823 K for 4 h. Most of the work was performed with the Degussa C-type alumina, which is a flame-hydrolyzed material with BET area near 97 m^2/g as supplied. The Alcoa alumina is a high surface area α-alumina (approximately 100 m^2/g as supplied). The alumina provided by Engelhard had been precalcined to BET areas of 62 and 21 m^2/g.

TABLE 1

Summary of Sample Pretreatments

Sample	Sample i.d.	Rh (wt%)	Alumina pretreatment	Alumina phase
Degussa C δ-Al_2O_3	D-1	0.60	873 K 4 h	δ-Al_2O_3
	D-2	0.54	1173 K 4 h	δ-Al_2O_3
	D-3	0.51	1273 K 4 h	δ-Al_2O_3
	D-4	0.48	1373 K 4 h	δ/θ-Al_2O_3
	D-5	0.20	1373 K 8 h	α/θ-Al_2O_3
	D-6	0.05	1373 K 24 h	α-Al_2O_3
	D-7	0.07	1423 K 4 h	α-Al_2O_3
Alcoa α-Al_2O_3	A-8	0.07	1173 K 4 h	α-Al_2O_3
Engelhard Al_2O_3	E-9	0.39	1323 K 4 h	θ/α-Al_2O_3
	E-10	0.13	1343 K 4 h	α/θ-Al_2O_3

Hydrothermally treated samples were prepared by subjecting a portion of each sample, formulated by the procedure above, to 10% H_2O in flowing air (200 cm^3/min) at 1223 K for 24 h. Hydrothermal treatment in air was employed as the exclusive aging environment because of the large number of studies (1–16) showing the strong deactivating impact of high-temperature oxidative treatments. High-temperature reducing treatments have been shown to reverse the effects of high-temperature oxidative treatments (1, 8, 12, 15), and were used in the present study in combination with temperature-programmed reduction to assess the amount of Rh that interacts strongly with the support. Beck and Carr (15) have carried out a study of Rh/Al_2O_3 aging in both oxidizing and reducing atmospheres, as well as in alternating oxidizing and reducing environments. They found that aging in oxygen at 1073 K decreased the apparent Rh dispersion more than any other aging mode.

The approach outlined above, starting with air aged alumina, loading with Rh, and subsequently aging at 1223 K in a hydrothermal environment, is designated scheme 1 in Figure 1. During the course of the study it became apparent that surface areas of the aluminas were changing during the hydrothermal aging. For this reason, some experiments were also carried out on samples aged by scheme 2 described in Figure 1. The only difference between the two preparative schemes was the insertion of an additional 24 h, 1223 K hydrothermal aging step for the furnace-aged alumina prior to impregnation of Rh.

X-Ray Diffraction (XRD)

XRD measurements were performed on the Al_2O_3 after the heat treatments to determine the alumina phases. XRD patterns were recorded on a Philips X-ray generator with a Debye–Scherrer camera. Cu$K\alpha$ X-rays (λ = 1.5418 Å) were used as the X-ray source. The XRD apparatus used to analyze the samples has been described in detail previously (17).

BET Surface Area

Surface areas of the furnace-aged Al_2O_3 starting material were measured to determine the required Rh loading levels. Surface area measurements were also made on the catalysts after hydrothermal aging. The surface areas were determined by the BET technique, employing nitrogen adsorption at liquid nitrogen temperature, with a Micromeritics instrument.

CO–H_2 Titration

A CO–H_2 titration method (i.e., methanation) (18, 19) was used to determine Rh dispersion on the Al_2O_3 support. A small amount (approximately 0.1 g) of each sample was packed in a glass U-tube in a "sandwich" of quartz wool. Each sample was oxidized in flowing O_2 (40 cm^3/min) for 30 min at 673 K and then reduced at 673 K in flowing H_2 (40 cm^3/min) for 30 min. After cooling the sample to room temperature in flowing H_2, two CO pulses of 2 cm^3 each were introduced to the sample with H_2 as a carrier gas. The sample was purged with H_2 for 10 min. The reactor tube was then sealed by closing three-way valves to trap the H_2 and the adsorbed CO. The sample was then heated at 673 K for 30–45 min to hydrogenate the adsorbed CO to form methane. The amount of CH_4 formed after the reaction was measured by a flame ionization detector on a Varian Star 3400 gas chromatograph.

The estimated noble metal dispersions are based on the assumed ratio of

$$Rh_{\text{surface atoms}} : CO_{\text{adsorbed}} : CH_{4\text{formed}} = 1.$$

Previous studies (18, 19) have shown that the assumed ratio of one methane molecule formed per CO molecule adsorbed is accurate. However, the assumed ratio of one CO molecule adsorbed per Rh surface atom is simply an estimate because of uncertainties in both the average bonding configuration of CO (i.e., linear, bridged, or dicarbonyl) and the saturation coverage. Thus all dispersions reported are apparent values based on the assumptions above, and the dispersion data are used simply as a rough estimate (to within about a factor of two) of the actual fraction of exposed Rh atoms.

Temperature-Programmed Reduction

TPR experiments were carried out on an Altamira temperature-programmed system. The details of the TPR apparatus have been reported elsewhere (17). Oxidizing pretreatments were carried out in the TPR cell in a 40 cm^3/min flow of 10% O_2 in He at 873 K for 50 min. The samples were cooled in O_2 to 277 K before the start of the temperature-programmed reduction. The samples were heated in 9% H_2 in Ar to 873 K at a rate of either 15 or 30 K/min and the H_2 consumption was monitored with a thermal conductivity detector. High-temperature reductions were performed on some of the hydrothermally aged catalysts (H_2 (40 cm^3/min) at temperatures between 1073 and 1123 K for 1 h) to reverse the strong interaction between the Rh and the Al_2O_3 support. This was followed by another oxidizing pretreatment and TPR as above.

RESULTS

Characterization of Alumina Phases

XRD was used to analyze the alumina phases obtained after heat treatment (Table 1). XRD revealed that Degussa C was predominantly δ-phase both as received and after heat treatment at 873 K for 4 h. The Degussa C material remained as predominantly δ-phase, up until about 1373 K, and then transformed to the α-phase over a narrow temperature range between 1373 and 1423 K. The furnace-aged Degussa alumina that was used to make samples D-6 and D-7 showed X-ray lines characteristic of α-alumina only.

The surface area of the Alcoa α-alumina decreased rapidly from a starting value near 100 m^2/g in the fresh state to levels near 10 m^2/g after a relatively mild furnace aging at 1173 K for 4 h as shown in Fig. 2. Subsequent furnace aging at temperatures up to 1473 K and/or hydrothermal aging at 1223 K for 24 h resulted in further loss in BET area to 4–7 m^2/g, essentially equivalent to the BET areas of the other α-aluminas prepared from the amorphous aluminas.

The Engelhard alumina samples, heat treated at 1323 and 1343 K, showed a mixture of θ- and α-phases as did the Degussa C sample D-5.

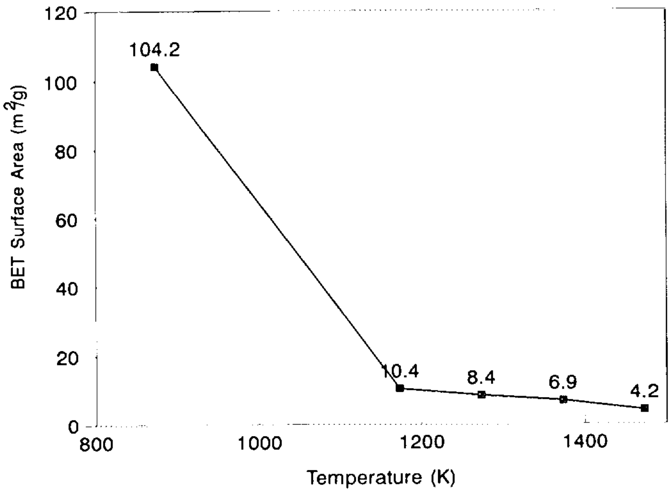

FIG. 2. BET surface area of Alcoa α-alumina as a function of aging temperature (for variable times) in air.

In all cases, 1223 K/24 h hydrothermal aging led to a decrease in BET area beyond that effected by the initial furnace aging. These results are shown in Table 2, where a comparison of fresh and steam aged BET areas is given. Fresh, in this case, refers to the alumina samples as freshly prepared by furnace aging in air. While the incremental BET surface area loss due to hydrothermal aging is not surprising for the samples that were initially aged in air at temperatures below 1223 K, it is somewhat surprising for the samples that were aged at temperatures up to 1423 K, such as D-7. Part of the reason for the incremental surface area loss upon hydrothermal aging are likely the longer times employed in hydrothermal aging compared to the initial furnace aging. However, even for a sample such as D-6 which was initially aged for 24 h at 1373 K, the additional 24-h hydrothermal aging at 1223 K resulted in further decrease in BET area from 8.4 to 6.6 m^2/g.

TABLE 2

BET Surface Area, Rh Loading, and Dispersion of Fresh and Steam Aged Samples (Scheme 1 Aging)

Sample	Rh Loading (wt%)	BET Surface area (m^2/g)		Dispersion (%)	
		Fresh	Steam aged	Fresh	Steam aged
D-1	0.60	96.6	77.0	65.2	4.5
D-2	0.54	86.6	75.9	62.8	5.2
D-3	0.51	82.1	73.4	56.1	5.2
D-4	0.48	76.4	56.6	58.7	4.9
D-5	0.20	32.7	14.6	42.4	3.3
D-6	0.05	8.4	6.6	48.7	10.1
D-7	0.07	11.3	7.2	57.1	9.9
A-8	0.07	10.4	6.4	53.2	5.2
E-9	0.39	62.0	40.0	37.9	2.6
E-10	0.13	21.0	10.0	41.6	1.0

Since Rh was impregnated onto the aluminas between the initial furnace aging and the subsequent hydrothermal aging, a possible explanation for the additional surface area loss caused by the hydrothermal aging is that the Rh promotes loss of surface area. To test this possibility, a sample of furnace-aged alumina was subjected to hydrothermal aging without the addition of Rh. The decrease in BET area was essentially identical to that of a correspondingly treated alumina sample which contained Rh. Thus Rh does not appear to accelerate the sintering of alumina in the hydrothermal treatment at 1223 K. We conclude, therefore, that the combination of the steam environment and the longer times accounts for the incremental surface area loss of these alumina samples.

Rh Dispersion

Table 2 lists the apparent Rh dispersion for each sample, both as initially prepared and after the standard 1223 K/24 h hydrothermal aging treatment. The purpose of the hydrothermal aging was to simulate high-temperature oxidative deactivation of Rh/alumina catalysts as it occurs in automotive exhaust.

In all cases, the percentage dispersion dropped dramatically after hydrothermal aging. However, with the exception of the Alcoa α-alumina, samples prepared on aluminas that had very low initial BET surface area and that showed only α-phase features in XRD, namely D-6 and D-7, yielded higher Rh dispersions (10.1 and 9.9%, respectively) than the samples with higher surface areas. Short of reaching an alumina structure that was predominantly α-phase, no trend in Rh dispersion was observed with decreasing surface area and/or change in phase structure from δ- to θ-phase.

Reducibility

TPR is a useful tool for gauging the fraction of Rh that has strongly interacted with the alumina after high-temperature oxidative treatments (1, 8). Selected samples of the Rh-impregnated aluminas were subjected to TPR as prepared, after hydrothermal aging, and after a so-called "restoration" treatment in flowing hydrogen at 1073–1123 K for 1 h. The high-temperature reduction has been shown to result in almost complete transformation of the Rh from a form that is strongly interacting with the alumina (i.e., not reducible at temperatures below about 873 K (20)) to a weakly interacting form with oxidation/reduction characteristics close to those of metallic Rh particles (8). This is clearly illustrated for the D-1 sample in Fig. 3. The freshly prepared, calcined sample gave a

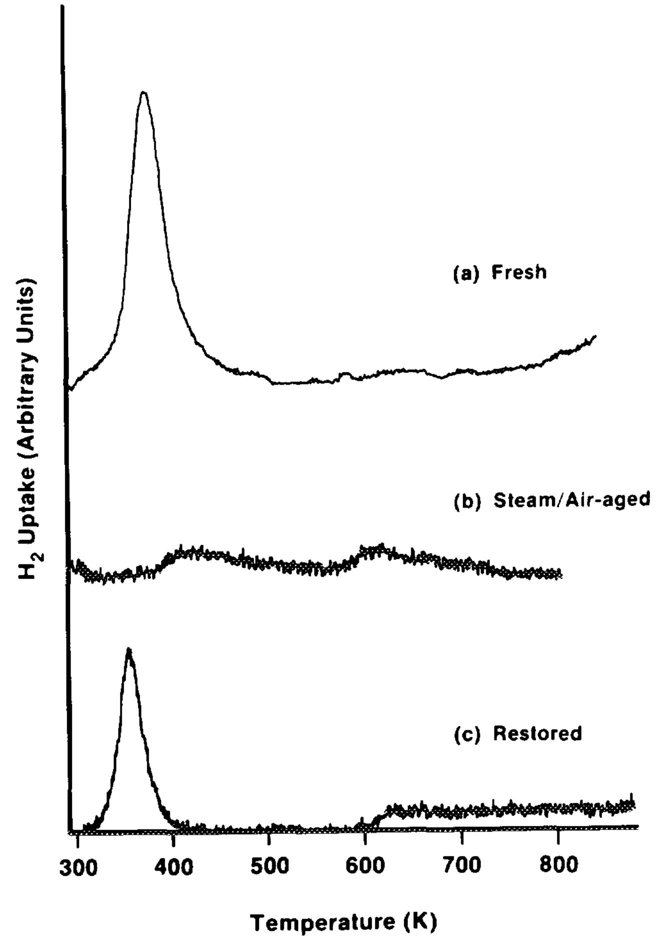

FIG. 3. TPR profiles of the D-1 Rh catalyst (prepared by scheme 1): (a) fresh, (b) 24 h hydrothermally aged, and (c) restored.

relatively sharp TPR peak centered at 360 K (Fig. 3a). After 1223 K hydrothermal aging the TPR peak nearly disappeared (Fig. 3b), indicating strong interaction of the Rh with the alumina support. After an 1123 K 1 h reduction and subsequent reoxidation, the Rh reduction peak reappeared as a relatively sharp feature at 340 K (Fig. 3c). Table 3 shows the integrated H_2 uptakes for the Rh reduction features in Figs. 3a–3c (scheme 1 aging). The hydrothermal aging decreased the amount of reducible Rh to about 20% of the theoretical maximum, assuming the reduction of Rh^{+3} to Rh^0. The subsequent high-temperature reduction treatment restored the amount of reducible Rh to about 40% of the theoretical value.

Note that the BET area of the D-1 sample dropped from 97 to 77 m^2/g during hydrothermal aging. To test whether this may have caused irreversible loss of accessible Rh, a second set of D-1 and D-7 samples were aged by scheme 2 and subsequently analyzed. Results are shown in Table 3. The additional hydrothermal aging carried out prior to Rh impregnation decreased the surface area of the D-1 alumina from 97 to 83 m^2/g and the surface area of the D-7 alumina from 11.3 to 8.5 m^2/g. For both the D-1 and D-7 samples, the aging by scheme 2 resulted in an almost complete accounting for the Rh by TPR after the restoration step. Thus, no more than about 5% of the Rh is irreversibly lost through loss of alumina surface area when a preliminary hydrothermal aging of the alumina is carried out prior to Rh impregnation and repeat hydrothermal aging.

Rh Loading Effect

A series of Rh catalyst samples of varying Rh loading were prepared on the Degussa D-7 α-alumina material and subjected to the standard 1223 K/24 h hydrothermal aging. The purpose of these experiments was to determine if the initial Rh loading affects the subsequent Rh dispersion after the high-temperature hydrothermal aging. As shown in Fig. 4, a strong effect was noted. At Rh loadings greater than about 1.5 $\mu mol/m^2$ (BET) the apparent Rh dispersion after hydrothermal aging was 3% or less. At loadings less than 1.5 $\mu mol/m^2$ (BET) the apparent dispersion after hydrothermal aging rose sharply to levels near 10% and remained relatively constant with decreasing Rh loading. Thus a maximum Rh loading of about 1 μmol/

TABLE 3

Properties of D-1 and D-7 Catalysts

Sample	BET area (m^2/g)	TPR H_2 uptake ($\mu mol/g$)[a]	Dispersion (%)	
			Apparent[b]	Effective[c]
D-1 (scheme 1)				
Fresh[d]	96.6	94.6	65.2	—
Steam aged	77.0	17.7	4.5	22.3
Restored	—	35.7	—	—
D-1 (scheme 2)				
Fresh[e]	82.5	73.5	37.9	—
Steam aged	76.4	33.0	6.1	13.7
Restored	—	71.3	13.1	13.8
D-7 (scheme 2)				
Fresh[e]	8.5	7.54	39.0	—
Steam aged	—	4.12	20.0	37.6
Restored	—	7.23	56.6	60.7

[a] Theoretical H_2 consumptions for samples D-1 (scheme 1), D-1 (scheme 2), and D-7 (scheme 2) are 87.8, 74.6, and 7.75 $\mu mol/g$, respectively. The theoretical H_2 consumption is based on $Rh_2O_3 + 3H_2 = 2Rh + 3H_2O$.

[b] Based on total Rh in sample.

[c] Based on fraction of noninteracted Rh in sample.

[d] Alumina pretreated according to Table 1 prior to Rh impregnation.

[e] Alumina pretreated according to Table 1 and subsequently hydrothermally aged at 1223 K/24 h prior to Rh impregnation.

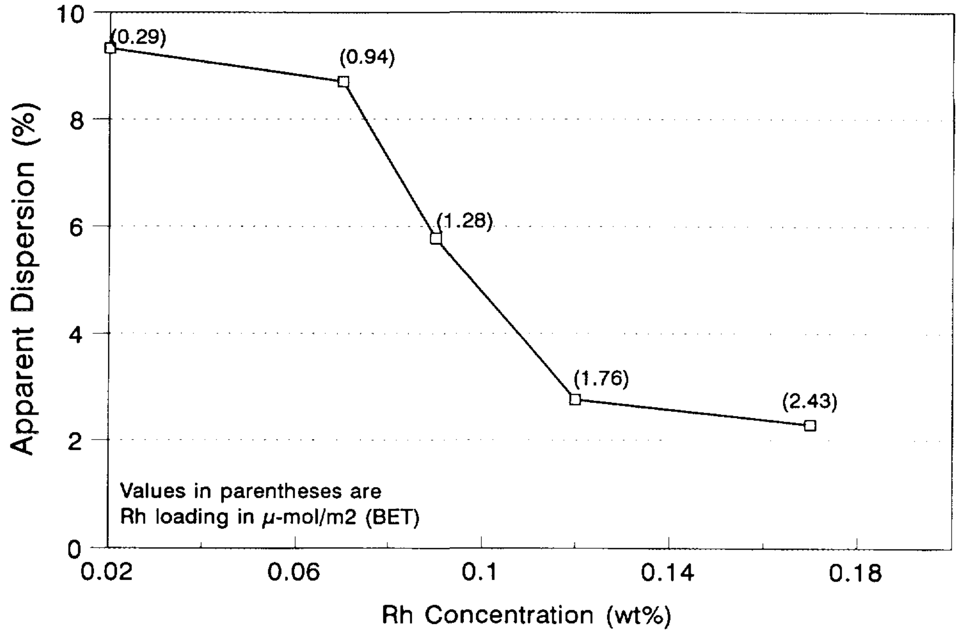

FIG. 4. Effect of loading on the apparent dispersion of Rh on α-alumina catalysts following 1223 K/24 h hydrothermal aging.

m^2 (BET) is defined, below which apparent dispersions ca. 10% can be obtained even after severe high-temperature hydrothermal aging.

Activity Measurements

Light-off tests were made on the D-1 catalyst and on the scheme 2 aged D-7 sample to test the effectiveness of the strategy of deploying Rh at low loadings on a presteamed α-alumina. The light-off experiments were carried out in a bench reactor at an effective lambda of 0.98 (i.e., slightly fuel-rich). The space velocity was set at 300 liter/h g for both catalysts, which required dilution of the D-1 sample with almost a tenfold excess of blank alumina to achieve equal charges of Rh (mass basis) to the reactor. The light-off curves are shown in Fig. 5. Temperatures of 50% conversion were significantly lower for the D-7 sample than for the D-1 sample at equivalent Rh charges to the reactor. Especially for NOx, the advantage of the α-alumina-based D-7 catalyst is strongly shown by its T_{50} of 723 K vs 793 K for the D-1 reference catalyst.

DISCUSSION

The results of this study indicate that low surface area aluminas, showing predominantly α-phase in XRD and 6–8 m^2/g BET area, are optimal for maximizing the amount of exposed Rh atoms after high-temperature oxidative treatments. The amount of exposed Rh is determined by three factors: (1) the extent of BET area loss during aging of the Rh-impregnated catalyst and associated *occlusion* of Rh particles, (2) the extent of *strong interaction* between the Rh and the support, and (3) the extent of *particle growth* (i.e., sintering) of the noninteracted/nonoccluded Rh. A similar partitioning has been alluded to by Beck and Carr (15) in an aging study of a 0.5% Rh/Al_2O_3 catalyst. However, the conditions of their aging experiments (1073 K maximum temperature for 4 h) were much milder than those reported here, resulting in much less irreversible loss of apparent Rh dispersion due to loss of alumina surface area.

Rh Partitioning after Aging

The relative contributions of the three factors listed above can be estimated from the combined TPR and CO-methanation data. The overall breakdown between *occluded*, *strongly interacted*, and *noninteracted* (i.e., reducible at temperatures below 873 K after high-temperature hydrothermal aging) Rh can be determined from the TPR H_2 uptakes measured for the fresh, hydrothermally aged, and restored samples. For example, Rh which is buried during collapse of the alumina pore structure cannot be subsequently oxidized and reduced, even after high-temperature reduction (restoration); thus, this fraction can be estimated from the difference between the amount of Rh measured by TPR in the fresh and restored samples. Similarly, the amount of noninteracted Rh is taken as that which is measured by TPR after hydrothermal aging, and the amount of strongly interacted Rh is taken as the difference between the Rh measured after

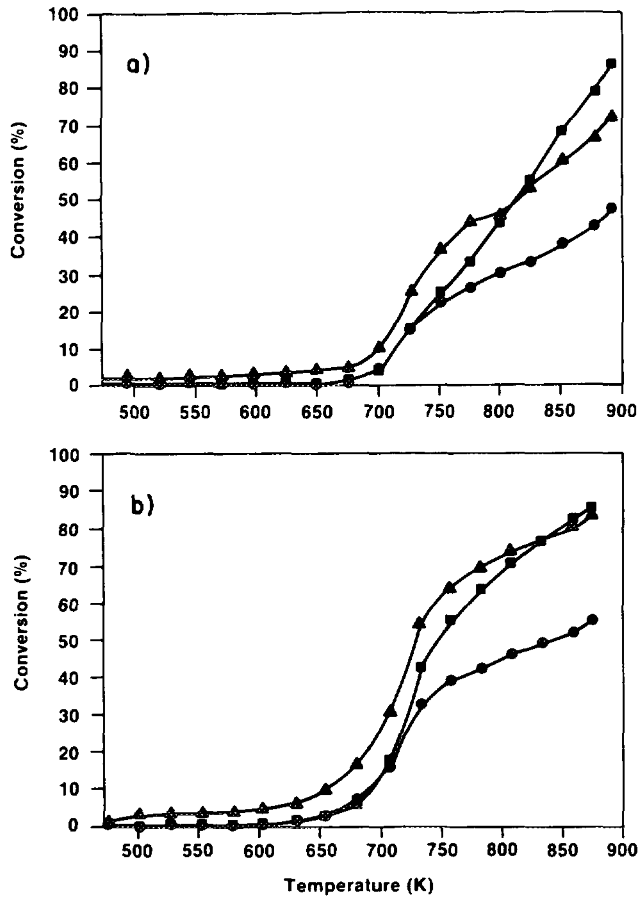

FIG. 5. Light-off plots for the scheme 1 aged D-1 (a) and scheme 2 aged D-7 (b) catalysts. D-1 (0.6% Rh) diluted nearly ten-fold with blank alumina to match total Rh content in the reactor with that of the D-7 sample (0.07% Rh). SV = 300 liter/h g λ = 0.98. Conversions are denoted as follows: triangles, NO; squares, propylene; circles, CO.

restoration and after high-temperature hydrothermal aging.

Following the scheme outlined above, Fig. 6 shows the distribution between the three types of Rh for the D-1 sample after both scheme 1 and scheme 2 aging. Scheme 1 aging results in occlusion of almost 60% of the Rh, despite the fact that the BET area decreased only from 96.6 to 77 m^2/g with hydrothermal aging. This fraction is dramatically reduced by going to scheme 2 aging where the alumina is hydrothermally aged prior to impregnation of the Rh (BET area = ~83 m^2/g). After the second hydrothermal aging the amount of occluded Rh decreased to about 4%. Correspondingly, the fractions of noninteracted and strongly interacted Rh are roughly equal and grow nearly proportionally as the amount of occluded Rh is decreased by scheme 2 aging.

Ultimately, the *fraction exposed* (i.e., dispersion) of the noninteracted Rh is a more important measure than simply the total amount of noninteracted Rh. These data are summarized for both theD-1 and D-7 samples in Table 3, both on an apparent basis (measured with respect to all of the Rh in the sample) and on an effective basis (measured with respect to the fraction of Rh in the noninteracted particles). Thus the complete breakdown for the scheme 2 aged D-1 sample is shown in Fig. 7a. Roughly 44% of the Rh remains noninteracted, of which 13.7% is present as exposed Rh atoms. In contrast, the scheme 2 aged D-7 sample (predominantly α-phase alumina) retains 53% of the Rh in a noninteracted form, of which 37.6% is present as exposed Rh atoms (Figure 7b). The overall utilization of Rh (equal to the apparent dispersion) is simply the product of the two fractions, i.e., 20% for the D-7 sample vs 6% for the D-1 sample. These results indicate more than threefold greater Rh utilization by deploying the Rh at low concentration (ca 0.05 wt%) over a large amount of low surface area, predominantly α-phase, alumina versus deploying it at high concentration (ca. 0.5 wt%) over a small amount of high surface area δ-phase alumina. Of course, the threefold greater Rh utilization factor is based on the assumption that the Rh particles in the two samples have roughly equivalent CO adsorption stoichiometries. However, even allowing for possible differences in adsorption stoichiometries, the much lower light-off temperatures observed for the scheme 2 aged D-7 catalyst provide independent evidence for more effective Rh utilization in the D-7 catalyst.

Loading Effect

Although detailed TPR measurements were carried out only for the D-1 and D-7 samples, it is clear from the CO/H_2 titration data of Table 3 that only those samples which combined low Rh loading and predominantly α-phase alumina yielded apparent dispersions in the range of 10%. The strong loading effect for the Rh on α-alumina catalysts (Fig. 4) suggests a critical initial concentration of Rh (ca. 1 μmol/m^2 (BET)) below which Rh can effectively be maintained at a factor of 3–5 higher dispersion than can be maintained at higher concentrations. Previous studies

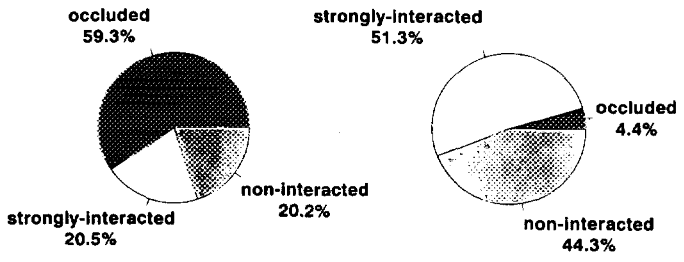

Scheme 1 Aging

Scheme 2 Aging

FIG. 6. Distribution of Rh in the D-1 catalyst after scheme 1 and scheme 2 aging.

a) D-1 Sample

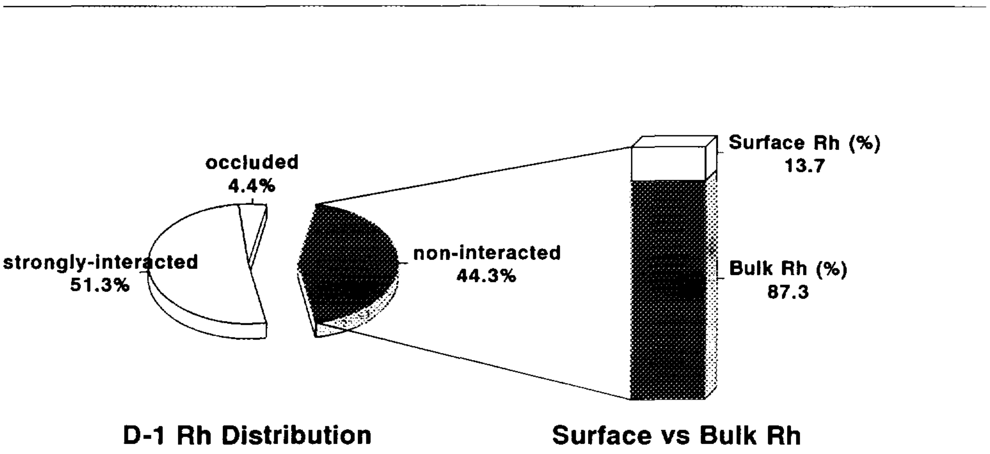

b) D-7 Sample

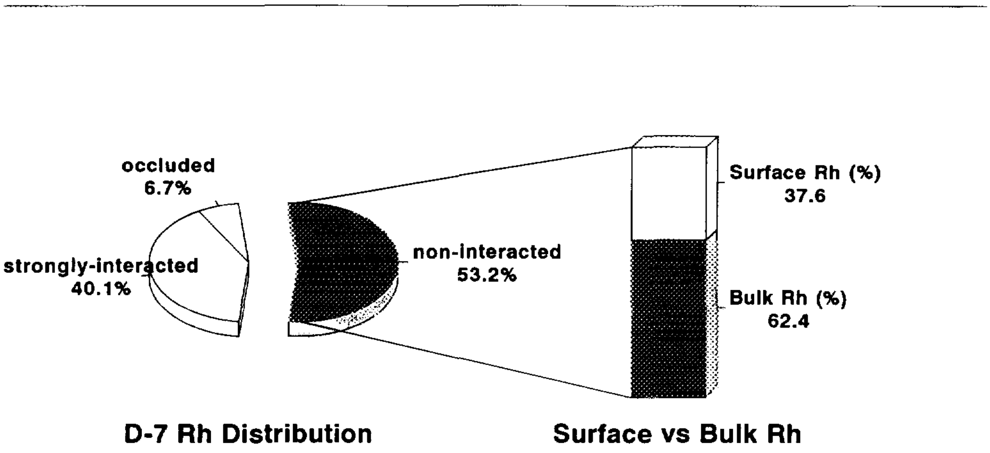

FIG. 7. Distribution of Rh in the D-1 (a) and D-7 (b) catalysts after scheme 2 aging. The distribution of Rh between surface and bulk in the noninteracted fraction of the Rh is also shown.

have shown a critical loading of 2.5 μmol of Rh/m^2 (BET) above which *fresh* (i.e., mildly calcined and reduced) samples show the nucleation of three-dimensional Rh particles (1). The two values are not directly comparable as the 1 μmol value relates to the ability of Rh to maintain dispersion in the face of severe thermal aging, while the 2.5 μmol value relates to the initial state of the catalyst after decomposition of the precursor species.

Analysis of the scheme 2 aged D-7 catalyst by transmission electron microscopy revealed mostly 6-nm Rh particles spaced about 60 nm apart (in two-dimensional projection). The alumina particles in the same sample are roughly 100 nm in diameter (from X-ray peak width analysis). Thus, to a first approximation, the Rh particle density in the loading range below 1 μmol/m^2 (BET) is about 1 Rh particle per alumina particle, suggesting that the Rh particle size is limited by the size of the alumina particle. In other words, sintering of the Rh on a given alumina particle is essentially complete but Rh does not move from alumina particle to alumina particle.

Nature of the Rh–Alumina Interaction

The nature of the strong interaction between Rh and alumina, which occurs in high-temperature oxidative environments, is not well understood, despite considerable study (7, 8). The present study employs techniques (TPR and CO/H$_2$ titration) that can only indirectly probe the nature of this interaction. However, the combined TPR and chemisorption data of Table 3 support the idea that the interaction involves a reversible encapsulation (or decoration) of Rh oxide particles by the alumina support. In Table 3, the key observation is that the effective dispersions of *both* the hydrothermally aged and restored D-1 samples are identical at about 14%. Thus, hydrothermal aging creates Rh particles that are on average about 14%

dispersed. About half of these particles interact with the support in such a way that they are rendered irreducible (below 873 K) and incapable of chemisorbing CO. The other half retain their reducibility and chemisorption capability. Since restoration does not change the effective dispersion, the picture that emerges is that particles stay intact during the process of interacting strongly with the support and undergoing subsequent restoration. This scenario is consistent with the recent EXAFS study of Beck *et al.* (7), which showed no evidence for coordination between Rh(III) and Al(III) cations at radial distances characteristic of either spinel structures or dissolution of Rh into the bulk. The D-7 catalyst showed a slightly different trend. The effective dispersion after hydrothermal aging was about 38% and increased to 61% after restoration, indicating some change in either particle size or morphology for the α-alumina-supported Rh.

Since Rh oxide particles (both amorphous and crystalline) are readily reduced to Rh metal in H_2, the inability to reduce them after high-temperature hydrothermal aging suggests that the H_2 is physically blocked from reaching the particles, presumably by a process of encapsulation or passivation by a thin film of aluminum oxide. The observation that only about half of the Rh oxide particles strongly interact with the support suggests that only certain crystal orientations of the rhodium oxide/aluminum oxide interface are conducive to the aluminum oxide migration required for encapsulation.

CONCLUSION

The following observations have been made on the effect of alumina phase structure on the utilization of Rh after high-temperature hydrothermal aging of Rh/Al_2O_3 catalysts:

1. The α-phase of alumina appears optimal for maximizing the dispersion of Rh after high-temperature steam/air aging. Apparent dispersions measured on α-Al_2O_3 were three- to fivefold higher than those measured on the transitional aluminas.
2. Presteaming the various alumina samples at 1223 K for 24 h prior to Rh impregnation resulted in additional BET surface area loss, even for those aluminas which initially had been furnace aged (dry) to obtain low surface areas.
3. Presteaming the aluminas prior to Rh deposition virtually eliminated irreversible occlusion of Rh by the alumina during subsequent high-temperature hydrothermal aging.
4. Loading Rh on α-alumina at concentrations less than about 1 μmol/m^2 (BET) resulted in three- to fourfold higher Rh dispersion after hydrothermal aging than obtained with higher loadings (>1.5 μmol/m^2 (BET)).
5. The combined effects of (1) using α-alumina for a catalyst support, (2) steam/air aging the alumina at high temperature prior to Rh deposition, and (3) loading Rh at levels below 1 μmol/m^2 (BET) result in a catalyst which is significantly more active than Rh deposited on higher surface area transitional aluminas (e.g., 90+ m^2/g δ-phase alumina), particularly aluminas that are not presteamed prior to Rh deposition.

ACKNOWLEDGMENTS

The authors appreciate the assistance of the late C. R. Peters in providing the X-ray identification of the alumina phases. We also thank R. Rajaram for coordinating the activity testing at the Johnson Matthey Sonning Research Center and E. Gulari for coordinating the microscopy work at the University of Michigan.

REFERENCES

1. Yao, H. C., Japar, S., and Shelef, M., *J. Catal.* **50,** 407 (1977).
2. Yao, H. C., Stepien, H. K., and Gandhi, H. S., *J. Catal.* **61,** 547 (1980).
3. Gandhi, H. S., Shelef, M., Yao, H. C., Kummer, J. T., and Stepien, H. K., U.S. Patent 4,172,047, October 23, 1979.
4. Koberstein, E., Society of Automotive Engineers, Paper 770366 (1977).
5. Cooper, B. J., Harrison, B., Shutt, E., and Lichtenstein, I., Society of Automotive Engineers, Paper 770367 (1977).
6. Duprez, D., Delahay, G., Abderrahim, H., and Grimblot, J., *J. Chim. Phys.* **83,** 465 (1986).
7. Beck, D. D., Capehart, T. W., Wong, C., and Belton, D. N., *J. Catal.* **144,** 311 (1993).
8. Wong, C., and McCabe, R. W., *J. Catal.* **119,** 47 (1989).
9. Kiss, J. T., and Gonzalez, R. D., *Ind. Eng. Chem. Prod. Res. Dev.* **24,** 216 (1985).
10. Yates, D. J. C., and Prestridge, E. B., *J. Catal.* **106,** 549 (1987).
11. Fiedorow, R. M. J., Chahar, B. S., and Wanke, S. E., *J. Catal.* **51,** 193 (1978).
12. Summers, J. C., and Ausen, S. A., *J. Catal.* **58,** 131 (1979).
13. Duprez, D., Barrault, J., and Geron, C., *Appl. Catal.* **37,** 105 (1988).
14. Chen, J. G., Colaianni, M. L., Yates, J. T., Jr., and Fisher, G. B., *J. Phys. Chem.* **94,** 5059 (1990).
15. Beck, D. D., and Carr, C. J., *J. Catal.* **144,** 296 (1993).
16. Gandhi, H. S., Kummer, J. T., Shelef, M., Stepien, H. K., and Yao, H. C., U.S. Patent 4,233,189, November 11, 1980.
17. Usmen, R. K., McCabe, R. W., Graham, G. W., Weber, W. H., Peters, C. R., and Gandhi, H. S., Society of Automotive Engineers, Paper 922336 (1992).
18. Komai, S., Hattori, T., and Murakami, Y., *J. Catal.* **120,** 370 (1989).
19. Usmen, R. K., McCabe, R. W., and Shelef, M., *in* "Proceedings of the Third Congress on Automotive Pollution Control," Elsevier, Brussels, Belgium, to be published.
20. Wong, C., and Tsang, C. M., Society of Automotive Engineers, Paper 922376 (1992).